Na+–Cl− ion pair association in supercritical water

A. A. Chialvo, P. T. Cummings, H. D. Cochran, J. M. Simonson, and R. E. Mesmer

Citation: The Journal of Chemical Physics **103**, 9379 (1995); doi: 10.1063/1.470707
View online: http://dx.doi.org/10.1063/1.470707
View Table of Contents: http://scitation.aip.org/content/aip/journal/jcp/103/21?ver=pdfcov
Published by the AIP Publishing

Articles you may be interested in

On the influence of the ionic charge on the mean force potential of ionpairs in water
J. Chem. Phys. **104**, 7219 (1996); 10.1063/1.471434

Influence of a nonionic surfactant on the rheology of a hydrophobically associating water soluble polymer
J. Rheol. **40**, 441 (1996); 10.1122/1.550753

Theory and modeling of ion–molecule radiative association kinetics
J. Chem. Phys. **104**, 4502 (1996); 10.1063/1.471201

Computer simulations of NaCl association in polarizable water
J. Chem. Phys. **100**, 3757 (1994); 10.1063/1.466363

Temperature dependence of interactions of an ion pair in water: A molecular dynamics study
J. Chem. Phys. **97**, 1919 (1992); 10.1063/1.463128

This article is copyrighted as indicated in the article. Reuse of AIP content is subject to the terms at: http://scitation.aip.org/termsconditions. Downloaded to IP: 137.189.170.231 On: Tue, 23 Dec 2014 10:29:41

Na^+–Cl^- ion pair association in supercritical water

A. A. Chialvo and P. T. Cummings
Department of Chemical Engineering, University of Tennessee, Knoxville, Tennessee 37996-2200 and Chemical Technology Division, Oak Ridge National Laboratory, Oak Ridge, Tennessee 37831-6268

H. D. Cochran
Chemical Technology Division, Oak Ridge National Laboratory, Oak Ridge, Tennessee 37831-6268

J. M. Simonson and R. E. Mesmer
Chemical and Analytical Science Division, Oak Ridge National Laboratory, Oak Ridge, Tennessee 37831-6110

(Received 10 July 1995; accepted 30 August 1995)

Molecular dynamics simulations of supercritical electrolyte solutions with three different ion–water models are performed to study the anion–cation potential of mean force of an infinitely dilute aqueous NaCl solution in the vicinity of the solvent's critical point. The association constant for the ion pair Na^+/Cl^- and the constant of equilibrium between the solvent-separated and the contact ion pairs are determined for three models at the solvent critical density and 5% above its critical temperature. The realism of the aqueous electrolyte models is assessed by comparing the association constants obtained by simulation with those based on high temperature conductance measurements. Some remarks are given concerning the calculation of the mean-force potential from simulation and the impact of the assumptions involved. © *1995 American Institute of Physics.*

I. INTRODUCTION

Solute speciation in near-critical aqueous electrolyte solutions plays an important role in industrial and natural chemical processes such as solid deposition[1] and metal corrosion[2] in steam cycles, solvent extraction,[3] crystal growth,[4] and hydrothermal ore formation.[5] Because the solvent's dielectric constant, to a large extent, regulates the water solvation power by screening the coulombic interactions,[6] aqueous electrolytes tend to associate at high temperatures and low densities, i.e., in the highly compressible region where the water dielectric constant diminishes dramatically with small perturbations of its state conditions.[7]

Our understanding of solute speciation at supercritical conditions is mostly based on conductimetric measurements of dilute aqueous alkali halides.[8,9] On the one hand, even though conductance measurements are quite challenging to perform at near-critical conditions, they provide not only a direct measure of the degree of association but also additional and useful information to rationalize experimental data from volatility,[10] isopiestic,[11] and calorimetric[12–14] measurements. On the other hand, while these static experimental methods yield comparable values for the association constant, they are less suited to offer insight into the structure and dynamics of the ion pairs. However, this can usually be remedied by the combination of the above static methods with dynamic ones such as those involving dielectric relaxation experiments.[15,16]

Ion association (speciation) has been typically studied through the definition of the association (dissociation) constant.[14,17] Although this is a common practice in the development of simple well-founded theoretical correlations for the thermodynamic properties of electrolyte solutions, it renders little insight into the mechanism of the speciation process. The main reason is that the theoretically calculated values of the association constant, and consequently the extent of the association, will depend on the realism embodied in the potential model used and on the accuracy (the approximations introduced in the formalism such as those related to the species activity coefficients) with which the theory represents such a model.[14,18] Alternatively, we can use molecular simulation techniques to study the structure and the energetic and dynamic nature of ion pairing in well-defined aqueous electrolyte models, and make contact between functionals of the solvent-averaged forces, such as the anion–cation potential of mean force, and either the association or equilibrium constant at near-critical conditions.

Several studies have been reported on the determination of the mean-force potential between aqueous ions at ambient conditions,[19–21] yet little is known about the speciation in aqueous solutions at near-critical and supercritical conditions[22,23] which are typically encountered in technological processes where supercritical water is either the reaction medium[24–26] or the energy carrier.[1] As part of a broader ongoing investigation of solvation at near-critical conditions, in this paper we report the molecular-based determination of the association and equilibrium constants for an infinitely dilute aqueous Na^+/Cl^- solution as described by three different water–electrolyte models at a supercritical state condition. In Sec. II we present the statistical mechanical formalism for the determination of the thermodynamic constants. In Sec. III we describe the three aqueous electrolyte models, the simulation methodology, and the resulting association and equilibrium constants. In Sec. IV we give some details on the conductance measurements and the resulting correlation for the association constant of NaCl, which is later used to test the realism of models in describing ion pairing at near-critical conditions. Finally, in Sec. V we discuss the outcome of the comparison between the association constants from simulation and experiment, the limitations of the present calculations regarding the constant of

This article is copyrighted as indicated in the article. Reuse of AIP content is subject to the terms at: http://scitation.aip.org/termsconditions. Downloaded to IP: 137.[illegible] On: [illegible]

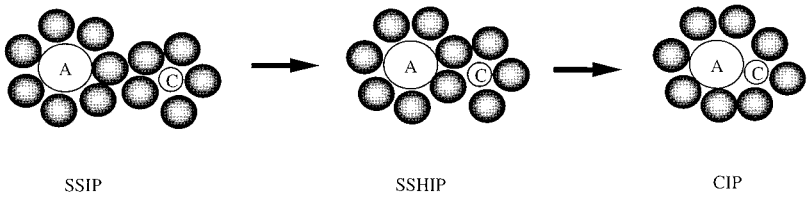

FIG. 1. Schematic of the SSIP, SSHIP, and CIP configurations.

integration, and the corresponding predictions of Bjerrum and Fuoss theories.

II. STATISTICAL MECHANICAL INTERPRETATION OF THE ASSOCIATION CONSTANT

Let us assume we have a dilute aqueous solution of a 1:1 salt composed of anions A and cations C in which the following chemical equilibrium takes place between the free ions, A and C, and the associated neutral pair AC. Because of the infinitely dilute conditions, we can assume that the association process involves only the formation of neutral pairs, i.e., no polyionic clusters,[27] through the following multistep mechanism:[28]

$$\underset{\text{free ions}}{\text{A}+\text{C}} \overset{K_1}{\Leftrightarrow} \underset{\text{SSIP}}{\text{A}\|\text{C}} \overset{K_2}{\Leftrightarrow} \underset{\text{SSHIP}}{\text{A}|\text{C}} \overset{K_3}{\Leftrightarrow} \underset{\text{CIP}}{\text{AC}}. \tag{1}$$

Thus, the equilibrium association constant can be expressed as,

$$K_a(T,\rho)=K_1(1+K_2+K_2K_3)=\frac{a_{\text{A:C}}}{a_{\text{A}}a_{\text{C}}}=\frac{[\text{A:C}]\gamma_{\text{A:C}}}{[\text{A}][\text{C}]\gamma_{\pm}^2}, \tag{2}$$

where a_i is the activity of the species i, A:C≡SSIP+SSHIP +CIP, $\gamma_{\text{A:C}}$ is the corresponding activity coefficient, $\gamma_{\pm}$ is the mean activity coefficient of the free ions in solution, and $[\cdots]$ denotes a molar concentration usually referred to in the literature as "c." Note that the association is depicted as a three-step process, involving the formation of the intermediates solvent-separated ion pair (SSIP, or loose ion pair),[29] solvent-shared ion pair (SSHIP), and contact-ion pair (CIP, or tight ion pair)[29] species.[6] This description is a little more detailed than the one usually found in the literature,[19,20] in that the ion pairs which are not CIP are split into SSHIP (only one layer of "sandwiched" water between the pair) and SSIP (more than one layer) as shown in Fig. 1.

By introducing the degree of dissociation α, Eq. (2) can be recast as,

$$K_a(T,\rho)=\frac{(1-\alpha)\gamma_{\text{A:C}}}{c\alpha^2\gamma_{\pm}^2} \tag{3}$$

or alternatively as,

$$K_a(T,\rho)=K_c(T,\rho)(\gamma_{\text{A:C}}/\gamma_{\pm}^2), \tag{4}$$

where K_c is the mass–action association constant.

To make the connection between the constants K_c and/or K_a and the solvation structure of the ion pair we rewrite these constants in terms of the actual number densities $\rho_i=N_i/V$, where N_i is the number of particles of species i and V is the total volume, as follows:

$$K_c=\frac{\rho_{\text{A:C}}}{\rho_{\text{A}}\rho_{\text{C}}}=\frac{(1-\alpha)}{\rho_0\alpha^2}, \tag{5}$$

where ρ_0 indicates the total (constant) number density of ions, i.e.,

$$\rho_{\text{A}}+\rho_{\text{A:C}}=\rho_{\text{C}}+\rho_{\text{A:C}}=\rho_0. \tag{6}$$

In the last term of Eq. (5) we have applied the species mass balance and the stoichiometry of the association reaction to relate the actual number densities (concentrations) to the degree of dissociation α, i.e.,

$$\rho_{\text{A:C}}=\rho_0(1-\alpha), \tag{7}$$

$$\rho_{\text{A}}=\rho_{\text{C}}=\rho_0\alpha. \tag{8}$$

In the statistical mechanical definition of anion–cation radial distribution function $g_{\text{AC}}(r)$ we have that,

$$N_{\text{A:C}}=4\pi\rho_0\int_{R_L<r<R_U} g_{\text{AC}}(r)r^2dr \tag{9}$$

is the average number of cations (C) within the anion (A) solvation shell of radius $R_L<r<R_U$ where R_L and R_U denote the lower and upper radial bounds for the solvation shell.

The choice of these bounds defines when a pair of ions is considered paired. Robinson and Stokes[30] stated that "the ion-pair must be long-lived enough to be a recognizable kinetic entity in the solution." In terms of structure this translates into finite contributions to the anion–cation pair distribution functions, with well-defined first and second peaks corresponding to the CIP and SSHIP configurations.

Now if we consider the cation–anion pair to be associated when the pair center-to-center separation r_{AC} is within a prescribed range, i.e., $R_L<r_{\text{AC}}<R_U$, then the number density of ion-pairs A:C is given by,[31]

$$\rho_{\text{A:C}}=4\pi\rho_0^2\int_{R_L<r<R_U} g_{\text{AC}}(r)r^2dr \tag{10}$$

and therefore, from Eqs. (7) and (10), the degree of dissociation becomes,

$$(1-\alpha)=4\pi\rho_0\int_{R_L<r<R_U} g_{\text{AC}}(r)r^2dr. \tag{11}$$

This article is copyrighted as indicated in the article. Reuse of AIP content is subject to the terms at: http://scitation.aip.org/termsconditions. Downloaded to IP:

Finally, from Eqs. (4) to (10) we have that the thermodynamic association constant is related to the anion–cation solvation structure as follows:

$$K_a=\left(4\pi\gamma_{A:C}\gamma_{\pm}^{-2}\int_{R_L<r<R_U}g_{AC}(r)r^2dr \Big/ \left(1-4\pi\rho_0\int_{R_L<r<R_U}g_{AC}(r)r^2dr\right)^2\right). \tag{12}$$

Note that Eq. (12) is valid for any total salt concentration ρ_0. However, because K_a is independent of composition and to avoid introducing unnecessary approximations for the species activity coefficients, we simplify its molecular-based calculation by analyzing the infinite dilute limit, $\rho_0\to 0$, i.e.,

$$K_a=4\pi\int_{R_L<r<R_U}g^{\infty}_{AC}(r)r^2dr \tag{13}$$

because the integral over the radial distribution function is finite,

$$\lim_{\rho_0\to 0}\rho_0\int_{R_L<r<R_U}g_{AC}(r)r^2dr=0 \tag{14}$$

and in the infinitely dilute limit,[32]

$$\lim_{\rho_0\to 0}\gamma_{\pm}^2=\lim_{\rho_0\to 0}\gamma_{A:C}=1, \tag{15}$$

where ∞ denotes an infinite dilution property. Note that from Eqs. (13) to (15) we also have that

$$\lim_{\rho_0\to 0}\alpha=1 \tag{16}$$

and therefore, that

$$\lim_{\rho_0\to 0}\left(\frac{1-\alpha}{\rho_0\alpha^2}\right)=K_a. \tag{17}$$

Similarly, we can define the constant of equilibrium between the SSIP and the CIP species, usually referred to as K_e, as follows:

$$K_e=(1/K_2K_3)=\frac{\rho_{SSIP}}{\rho_{CIP}} \tag{18}$$

which in terms of $g_{AC}(r)$ becomes,

$$K_e=\int_{R_L<r<R_U}g_{AC}(r)r^2dr \Big/ \int_{0<r<R_L}g_{AC}(r)r^2dr. \tag{19}$$

Likewise we could define the equilibrium constants K_1, K_2, and K_3 but they are of little interest for our purposes in this paper.

Note that, according to Eq. (12), for small salt concentrations for which we can assume that $\gamma_{\pm}^2\approx\gamma_{A:C}\approx 1$, the degree of dissociation is given by

$$\alpha=(1/2\rho_0K_a)[(1+4\rho_0K_a)^{0.5}-1]. \tag{20}$$

Therefore, for $\rho_0K_a\ll 1$, i.e., when $(1+4\rho_0K_a)^{0.5}\approx 1+2\rho_0K_a-2\rho_0^2K_a^2$ we have that,

$$\alpha\approx 1-\rho_0K_a. \tag{21}$$

Alternatively, for $\rho_0K_a\gg 1$ we have,

$$\alpha\approx(1/\rho_0K_a)^{0.5}. \tag{22}$$

Note also that Eq. (11) reduces to the Bjerrum expression[33] if we assume that the anion–cation mean-force potential $W_{AC}(r)=-kT\ln g^{\infty}_{AC}(r)$ is given by the dielectric-screened anion–cation electrostatic potential $\phi_{AC}(r)=q_Aq_C/\epsilon r$, where $R_L=a$ is the distance of closest ionic approach, and $R_U=r_{min}$ is the position of the minimum of the Boltzmann distribution, i.e., $r_{min}=-q_Aq_C/2kT\epsilon$ (for details see Fig. 8.1 of Marcus's book).[6]

III. INTERMOLECULAR POTENTIALS AND SIMULATION DETAILS

The main goal of this study is to find how sensitive the association constants are to the nature of the ion–water and anion–cation intermolecular potentials for a common water model. For the reason already mentioned in our earlier work[34,35] we use the simple point charge (SPC) water model throughout this work, i.e., the water–water interactions are described by,[36]

$$\phi_{WW}(\mathbf{r}_{12}\boldsymbol{\omega}_1\boldsymbol{\omega}_2)=\sum_{\alpha=1}^{3}\sum_{\beta=1}^{3}\frac{q_1^{\alpha}q_2^{\beta}}{r_{12}^{\alpha\beta}}+4\epsilon_{OO}\left[\left(\frac{\sigma_{OO}}{r_{OO}}\right)^{12}-\left(\frac{\sigma_{OO}}{r_{OO}}\right)^{6}\right], \tag{23}$$

where the subscript OO denotes oxygen–oxygen interactions, $\mathbf{r}_{12}$ is the vector joining the centers of molecules 1 and 2, $\boldsymbol{\omega}_i$ represents the orientational vector of molecule i, q_i^{α} is the charge on site α on molecule i, $r_{12}^{\alpha\beta}$ is the distance between site α on molecule 1 and site β on molecule 2, and ϵ and σ are the Lennard-Jones energy and size parameters, respectively.

Our study consists of simulations of three types of ion–water potential models, namely, Pettitt–Rossky's (PR),[37] Chandrasekhar *et al.*'s (CSJ),[38] and Pálinkás *et al.*'s (PRH).[39] The rationale for that choice is simple: we chose the first two models to keep consistency with our previous investigation of aqueous[35,40–42] and aqueous–organic electrolyte solutions.[43] The PRH model was chosen because it differs radically from the other two, especially in terms of the ion–ion pair interactions and ion–water combining rules, making it appropriate to analyze the impact of strength of the ion–ion interactions on the mean-force potential and related integrals.

The PR model describes each ion–water interaction as the sum of an ion–oxygen Lennard-Jones interaction plus the ion–oxygen and two ion–hydrogen Coulombic interactions, i.e.,

$$\phi_{IW}(\mathbf{r}_{IW}\boldsymbol{\omega}_W)=\sum_{\beta=1}^{3}\left\{\frac{q_Iq_W^{\beta}}{r_{I\beta}}+4\epsilon_{I\beta}\left[\left(\frac{\sigma_{I\beta}}{r_{I\beta}}\right)^{12}-\left(\frac{\sigma_{I\beta}}{r_{I\beta}}\right)^{6}\right]\right\}, \tag{24}$$

where ϵ_{IW} and σ_{IW} are given by the Lorentz–Berthelot combining rules in Table I.[44]

This article is copyrighted as indicated in the article. Reuse of AIP content is subject to the terms at: http://scitation.aip.org/termsconditions. Downloaded to IP:

TABLE I. Parameters of Pettitt–Rossky (PR) ion–water interactions.

Pair	$\epsilon_{I\beta}$ (ergs)	$\sigma_{I\beta}$ (Å)
Na^+–O	9.30×10^{-15}	2.72
Na^+–H	9.30×10^{-15}	1.31
Cl^-–O	2.50×10^{-14}	3.55
Cl^-–H	2.50×10^{-14}	2.14

For the ion–ion interaction, we use the Huggins–Mayer–Fumi–Tosi model for alkali–halide interactions,[45,46] i.e.,

$$\phi_{ij}(r)=\frac{q_iq_j}{r}+B_{ij}e^{-r/\rho_{ij}}-\frac{C_{ij}}{r^6}, \tag{25}$$

where B_{ij}, ρ_{ij}, and C_{ij} are ion-pair specific constants given in Table II.

The CSJ model[38] describes each ion–water interaction as the sum of an ion–oxygen Lennard-Jones plus the ion–oxygen Coulombic interactions, i.e.,

$$\phi_{\mathrm{IW}}(\mathbf{r}_{\mathrm{IW}}\boldsymbol{\omega}_{\mathrm{W}})=\sum_{\beta=1}^{3}\frac{q_{\mathrm{I}}q_{\mathrm{W}}^{\beta}}{r_{I\beta}}+4\epsilon_{\mathrm{IO}}\left[\left(\frac{\sigma_{\mathrm{IO}}}{r_{\mathrm{IO}}}\right)^{12}-\left(\frac{\sigma_{\mathrm{IO}}}{r_{\mathrm{IO}}}\right)^{6}\right], \tag{26}$$

where ϵ_{IO} and σ_{IO} are given by the Berthelot (geometric mean) combining rule in Table III.[44] Note that this model has been parametrized for the TIP4P water model and a Lennard-Jones anion–cation potential, while here it is used in conjunction with the SPC and the Huggins–Mayer–Fumi–Tosi models.

The PRH model[39] describes each ion–water interaction as the sum of ion–oxygen Lennard-Jones plus the ion–oxygen and ion–hydrogen Coulombic interactions, i.e.,

$$\phi_{\mathrm{IW}}(\mathbf{r}_{\mathrm{IW}}\boldsymbol{\omega}_{\mathrm{W}})=\sum_{\beta=1}^{3}\frac{q_{\mathrm{I}}q_{\mathrm{W}}^{\beta}}{r_{I\beta}}+4\epsilon_{\mathrm{IO}}\left[\left(\frac{\sigma_{\mathrm{IO}}}{r_{\mathrm{IO}}}\right)^{12}-\left(\frac{\sigma_{\mathrm{IO}}}{r_{\mathrm{IO}}}\right)^{6}\right], \tag{27}$$

where ϵ_{IO} and σ_{IO} are given by Kong's combining rules[47] in Table IV. Note that this model has been parametrized for the ST2 water model and a Lennard-Jones plus Coulombic anion–cation potentials. The ion–ion non-Coulombic interactions are modeled by a simple Lennard-Jones potential (Table IV).

The Newton–Euler equations of motion for water were integrated via Gear's fourth-order predictor–corrector algorithm[48] with a Gaussian thermostat, as described in greater detail elsewhere.[35] The constrained equations of motion for the ion pair were integrated with a velocity Verlet algorithm, coupled to the analytical solution of the constraint.[49] All simulations were performed in the canonical–isokinetic (NVT) ensemble, with $N=256$ particles—$N-2$ water molecules plus an anion and a cation—at the system density and temperature of $\rho=0.27$ g/cm^3 and $T=616$ K, respectively. The state condition corresponds to $T_r=1.05$, $\rho_r=1.0$ based on the critical conditions for the SPC water model.[50] Standard periodic boundary conditions were used along with the minimum image criterion, a spherical cutoff for the truncated intermolecular interactions, and a Verlet neighbor list.[51] Long-ranged Coulombic interactions were corrected by a molecular (center-to-center) and a site-to-site reaction field for the water–water and the ion–water interaction, respectively, with a dielectric constant $\epsilon_{\mathrm{rf}}=20$.[52] No long-range correction was introduced for the nonelectrostatic interactions. Each run was started from the previous equilibrated one, corresponding to a slightly different (0.2 Å) constrained pair distance. After a short (1000 time steps) equilibration to the new constrained pair distance, each production run comprised 1.5×10^5 time steps, with a time step size of 10^{-3} ps, divided into 10 subruns from which the averages and standard deviations were obtained.

TABLE II. Parameters of the Huggins–Mayer–Fumi–Tosi ion–ion interactions.

Pair	B_{ij} (ergs)	ρ (Å)	C_{ij} (ergs Å^6)
Na^+–Na^+	6.789×10^{-10}	0.317	1.684×10^{-12}
Na^+–Cl^-	2.015×10^{-9}	0.317	1.119×10^{-11}
Cl^-–Cl^-	5.575×10^{-9}	0.317	1.169×10^{-10}

TABLE III. Parameters of Chandrasekhar *et al.*'s (CSJ) ion–water interactions.

Pair	$\epsilon_{I\beta}$ (ergs)	$\sigma_{I\beta}$ (Å)
Na^+–O	3.464×10^{-14}	2.451
Cl^-–O	9.379×10^{-15}	3.739

A. Association and equilibrium constants from constraint molecular dynamics

According to the analysis of Sec. II the calculation of the equilibrium constants at infinite dilution reduces in practice to the determination of the anion–cation radial distribution function at infinite dilution. Since these thermodynamic constants are composition independent, their determination becomes simpler when done at infinite dilution because we avoid the problems associated with the evaluation of the species activity coefficients. However, this must be achieved at the expense of an adequate method for the accurate determination of the infinite dilution anion–cation radial distribution function $g_{\mathrm{AC}}^{\infty}(r)$.

Radial distribution functions are usually a by-product of the simulation, one based on the counting of pairs as a function of their separation during the force calculation. For highly dilute systems this method becomes impractical due to an obvious sampling deficiency, and the practical solution

TABLE IV. Parameters of Pálinkás *et al.*'s (PRH) ion–ion and ion–water interactions.

Pair	$\epsilon_{I\beta}$ (ergs)	$\sigma_{I\beta}$ (Å)
Na^+–Na^+	5.94×10^{-15}	2.73
Cl^-–Na^+	2.83×10^{-15}	3.87
Cl^-–Cl^-	2.79×10^{-15}	4.86
Na^+–O	7.59×10^{-15}	2.936
Cl^-–O	4.77×10^{-15}	4.011

This article is copyrighted as indicated in the article. Reuse of AIP content is subject to the terms at: http://scitation.aip.org/termsconditions. Downloaded to IP:

is the direct determination of the corresponding potential of mean force, $W_{AC}(r) = -kT \ln g^{\infty}_{AC}(r)$, by means of either a free energy[53] or a mean-force approach.[54] Though usually these two methods are considered as two different approaches, the latter is actually a special case of the former in that the free energy is determined via a thermodynamic integration (the coupling parameter is simply the radial distance), as opposed to a perturbation approach. In that sense, the constraint method might exhibit slightly better statistics than the perturbation method for reasons already discussed by Mezei and Beveridge.[55] If properly performed, both methods give the same result.[56]

The potential of the mean-force $W_{AC}(r)$ is the change of free energy for the process of bringing together the ion pair from an infinite distance where $W_{AC}(r \to \infty) = 0$ to the distance r, and is microscopically represented by the solvent-averaged structural effect on the anion–cation interactions. During the simulation run the mean force exerted by the solvent on the anion, $\mathbf{F}_{WA}$, and on the cation, $\mathbf{F}_{WC}$, are evaluated as time averages so that the solvent contribution to the anion–cation mean force becomes,

$$\Delta F(r) = 0.5 \langle \hat{r}_{AC} \cdot (\mathbf{F}_{WA} - \mathbf{F}_{WC}) \rangle, \tag{28}$$

where $\hat{r}_{AC}$ is the unit vector along the direction of the anion–cation interactions, and $\langle \cdots \rangle$ indicates a time average over the phase space trajectory. The integration of the total anion–cation mean force, $F(r) = -dW_{AC}(r)/dr$, i.e., the sum of $\Delta F(r)$ and the direct anion–cation Coulombic and non-Coulombic contributions $F^{d}_{AC}(r)$ finally gives the desired potential of mean force $W_{AC}(r)$, i.e.,

$$W_{AC}(r) = W_{AC}(r_0) - \int_{r_0}^{r} F(r) dr. \tag{29}$$

According to the physical meaning of $W_{AC}(r)$ the natural choice for the integration constant is $W_{AC}(r_0 \to \infty) = 0$, however, this is infeasible for finite-sized simulation systems. Here we adopt the standard practice[20,54] by assuming the continuum limiting behavior $W_{AC}(r_0) \approx (q_A q_C / \epsilon r_0)$ for $r_0 \approx 8.1$ Å, where ϵ is the macroscopic dielectric constant of the solvent as obtained by simulation at the same state conditions.[57] Therefore the calculation of $g^{\infty}_{AC}(r)$ in the range (1 Å$< r <$8.1 Å) involves a set of ~40 simulation runs, each covering 150 ps of phase-space trajectory.

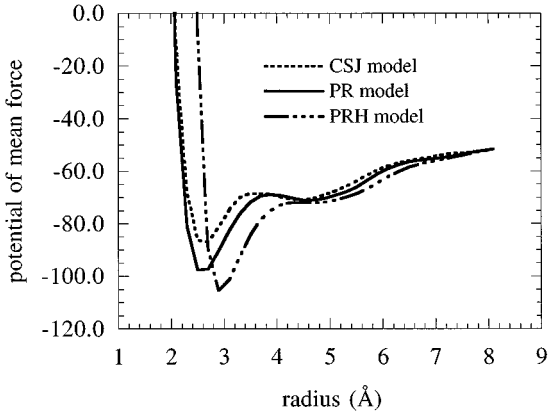

FIG. 3. Radial dependence of the potential of mean force in units of ϵ_{OO} ($1.079\,57 \times 10^{-14}$ ergs/molecule) for the Na^+–Cl^- pair interaction in SPC at $T_r = 1.05$, $\rho_r = 1.0$. A comparison between simulation results using PRH, PR, and CSJ models.

B. Simulation results for NaCl–water

In contrast to our earlier calculations[34,42] where we evaluated $W_{AC}(r_0)$ based on a less accurate value for the dielectric constant ($\epsilon \approx 8.8 \pm 0.9$ for SPC water at $\rho = 0.27$ g/cc and $T = 616$ K), here instead we use a new estimate, $\epsilon \approx 5.2 \pm 0.2$ (see Fig. 2) based on a simulation approximately 30 times longer than that reported earlier.[40]

In Fig. 3 we present the three resulting potentials of mean force from constraint dynamics simulation. The three models show qualitatively the same features, namely, two minima in the simulated mean-force potential corresponding to the CIP and SSHIP configurations, respectively. However, note that the second minimum of the PMF in the PRH model is rather a plateau with an inflection point at ~4.8 Å. The PR and the CSJ models predict similar PMFs, though the first model exhibits a deeper minimum at ~2.5 Å, indicative of a

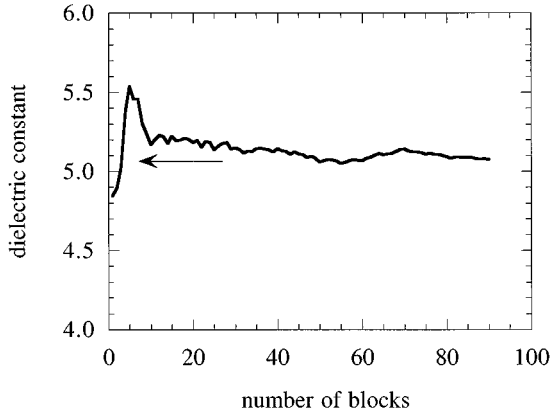

FIG. 2. Dielectric constant of SPC water at $T_r = 1.05$, $\rho_r = 1.0$ as a function of the number of averaging blocks. Each block comprises 10^4 time steps. The arrow indicates the experimental value (Refs. 7).

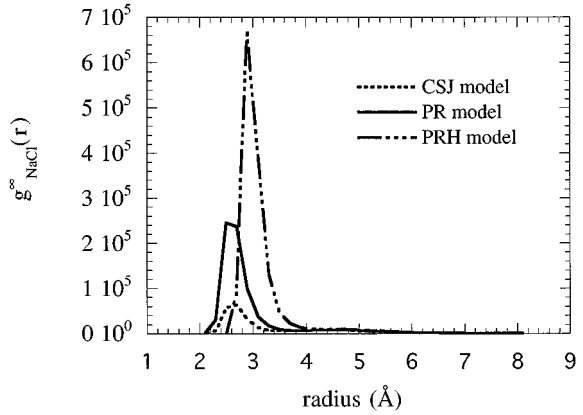

FIG. 4. Radial distribution function for the Na^+–Cl^- pair interaction in SPC at $T_r = 1.05$, $\rho_r = 1.0$. A comparison between simulation results using PRH, PR, and CSJ models.

This article is copyrighted as indicated in the article. Reuse of AIP content is subject to the terms at: http://scitation.aip.org/termsconditions. Downloaded to IP:

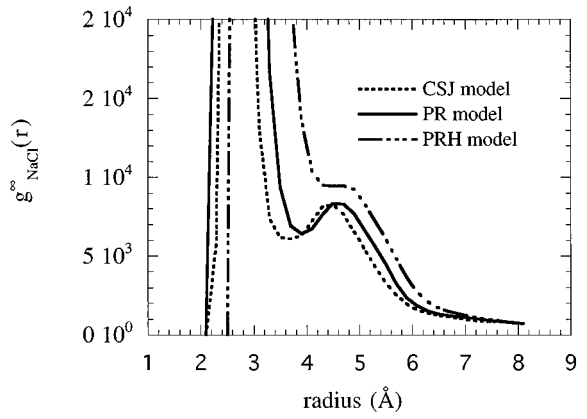

FIG. 5. Detailed view of the second peak of the radial distribution function for the Na^+–Cl^- pair interactions in SPC at $T_r=1.05$, $\rho_r=1.0$. A comparison between simulation results using PRH, PR, and CSJ models.

stabler CIP than that for the CSJ model. In Fig. 4 we compare the corresponding anion–cation radial distribution functions $g^{\infty}_{\mathrm{NaCl}}(r)$. This figure clearly shows the relative strength of the CIP configurations, i.e., the PRH model predicts the strongest while the CSJ model predicts the weakest CIP configuration, the latter being an order of magnitude smaller than the former. However, according to Fig. 5, the three models predict a remarkably similar strength for the SSHIP, especially the CSJ and the PR models.

Finally, the integration of Eqs. (13) and (19) gives the three sets of association and equilibrium constants as presented in Table V. The quoted errors in $\log K_a^M$ and $\log K_e$ have been obtained by a Monte Carlo method as described in the Appendix.

IV. CONDUCTANCE MEASUREMENTS FOR DILUTE NEAR-CRITICAL AQUEOUS NaCl SOLUTIONS

Electrical conductance measurements provide the most direct approach to the determination of the ion association constant at near-critical conditions for simple dilute aqueous electrolytes solutions, such as NaCl at high temperatures and pressures. The application of this technique to the determination of association constant at elevated temperatures and pressures has been recently reviewed.[14,58] Here we only summarize the main concept behind the method. The connection between the molar conductance Λ, the limiting conductance Λ_0, and the association constant in molar units K_a^M, is usually made (though not exclusively) through Shedlovsky's equation,[59]

$$\frac{1}{\Lambda S(z)}=\frac{1}{\Lambda_0}+\frac{MS(z)\Lambda\gamma_{\pm}^2}{K_a^M\Lambda_0^2}, \tag{30}$$

where M is the molarity, $\gamma_{\pm}$ is the corresponding mean-ionic activity coefficient, $S(z)=(1+z)$ is an empirical coefficient with $z=(\alpha\Lambda_0+\beta)\sqrt{M\Lambda/\Lambda_0^3}$ and $(\alpha\Lambda_0+\beta)$ denotes the limiting Onsager slope. The simultaneous solution of Eq. (30) for a set of conductance measurements over a range of state conditions and global compositions provides the values of Λ_0 and K_a^M. Finally $K_a^M(T,\rho)$ is regressed by a nonlinear least-square method.

Even though the ion-association constant of NaCl in aqueous solutions has been determined earlier from conductance measurements by Fogo *et al.*[60] and Quist and Marshall,[8] the recent calculations of Ho *et al.*[9] are better suited for a comparison with our simulation results because they involved measurements at more appropriate state conditions. Their regression results in the following temperature and density dependence for $\log K_a^M$:

$$\log\ K_a^M=0.997-650.07T^{-1}-(11.420-2600.5T^{-1})\log\ \rho, \tag{31}$$

where ρ is the solvent density in units of g/cc, T is the absolute temperature, and the superscript M denotes molarity. For water, at the state point treated in the simulation—$T_r=1.05$, $\rho_r=1.0$, i.e., $T=679.5$ K, $\rho=0.322$ g/cc—Eq. (31) predicts $\log K_a^M=3.78$ with an experimental uncertainty of $\delta\log K_a^M\approx\pm0.2$.[9]

V. DISCUSSION AND FINAL REMARKS

Our potential of mean-force calculation indicates that under the near-critical, highly compressible, and low dielectrically screened conditions studied here water is still a moderate solvent. In fact, the degree of dissociation α predicted by these models indicates that, at a molar salt concentration of 10^{-4} M (salt molar fraction $x_2\approx5.6\times10^{-6}$ at the specified water state conditions) for which we can presume the validity of the assumption behind Eq. (20), between 45% and 72% of all ion pairs are dissociated (see Fig. 6). As the total concentration decreases, α approaches unity as expected [see Eq. (16)], i.e., complete dissociation. In contrast, at ambient conditions, at a concentration as low as 10^{-4} M the dissociation is practically complete, i.e., $\alpha>0.999$.[19]

Before drawing any conclusions from the comparison between the simulation results and experimental values of the association constant, we must recognize the sources of uncertainties and the assumptions involved in the working expressions. Obviously, the constant of integration $W_{\mathrm{AC}}(r_0)$ in Eq. (29) introduces the largest source of error, i.e.,

$$g^{\infty}_{\mathrm{AC}}(r)=\exp(-\beta q_{\mathrm{A}}q_{\mathrm{C}}/r_0\epsilon)\vartheta_{\mathrm{AC}}(r),\quad 0<r<r_0, \tag{32}$$

TABLE V. Simulation results for association and equilibrium constants at $\rho_r=1$ and $T_r=1.05$.

Model	CIP (%)	$\log K_a^M$	$\log K_e$	R_L (Å)	R_U (Å)
PRH	87.	4.36±0.04	−0.84±0.02	4.5	8.1
PR	72.	4.03±0.04	−0.38±0.02	3.9	8.1
CHJ	45.	3.71±0.03	0.08±0.02	3.7	8.1

This article is copyrighted as indicated in the article. Reuse of AIP content is subject to the terms at: http://scitation.aip.org/termsconditions. Downloaded to IP:

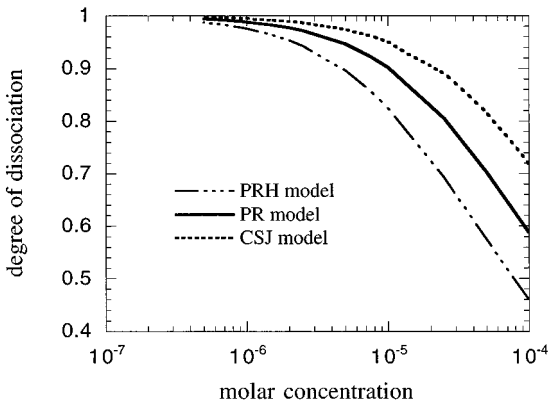

FIG. 6. Degree of dissociation as a function of the salt molar concentration as predicted by the association constant using PRH, PR, and CSJ models at $T_r=1.05$, $\rho_r=1.0$.

where $\vartheta_{\mathrm{AC}}(r) = \exp[\beta\int_{r_0}^{r} F(s)ds]$, associated with the uncertainty involved in the evaluation of the solvent's dielectric constant. In fact, a few percent uncertainty in this property will have an exponential impact on the value of the association constant. (Note that this will not be the case for the constant of equilibrium K_e). This, in turn, may obscure the test of the realism of the model by either canceling or magnifying errors in the calculation of the association constants. Even when a very accurate value for the model solvent's dielectric constant is available at the corresponding reduced state conditions (T_r and ρ_r), there will be always a source of ambiguity in the comparison, unless the critical conditions of the model coincide with those of the real solvent, because ϵ in $W_{\mathrm{AC}}(r_0)$ appears as the product $\epsilon\, T \equiv \epsilon(T/T_c, \rho/\rho_c)\, T$.

We have recently discussed[34] that an effective way to overcome the difficulties associated with $W_{\mathrm{AC}}(r_0)$ is to make the comparison between simulation and experimental values for the portion of K_a related to the integral in Eq. (29), i.e.,

$$I_a = 4\pi \int_0^{R_U} \vartheta_{\mathrm{AC}}(r) r^2 dr \tag{33}$$

rather than the values of the K_a's themselves. The integrand of Eq. (33) depends explicitly on the microscopic details (strength and nature) of the ion–ion and ion–solvent interactions as well as on the state conditions. In fact, for an infinitely dilute supercritical aqueous solution of NaCl, Cui and Harris results[22] indicate that $\log I_a \approx 4.3 \pm 0.13$ at $\rho=0.1252$ g/cc and $T=700$ K, as well as $\log I_a \approx 5.6 \pm 0.13$ at $\rho=0.0832$ g/cc and $T=800$ K. Moreover, from simulation results of Dang *et al.*[19] for the same system at ambient conditions we have that $\log I_a \approx -2.76$, in comparison to $\log I_a \approx -1.38$ for the same system but with the flexible rather than the rigid SPC water model.[20]

From the experimental value of $\log K_a^M = 3.78 \pm 0.2$, assuming $r_0 = 8.1$ Å, $\epsilon(T_r=1.05, \rho_r=1) \approx 5.1$, and the corresponding critical conditions for real water,[7] we obtain $\log I_a \approx 1.20 \pm 0.2$. This value is compared with the corresponding simulation results of the three models in Table VI.

From the analysis of Table V and the experimental result of K_a^M [Eq. (31)] we would have concluded that the best agreement between experiment and simulation—the most realistic model representation for ion pairing—is given by the CSJ model. However, this agreement comes as a result of a fortuitous compensation between $W_{\mathrm{AC}}[r_0, \epsilon(T_r, \rho_r), T]$ and I_a. In fact, if we make the direct comparison between I_a values from experiment and simulation, Table VI, the CSJ model predicts an integral I_a which is 30% smaller than that from experiment. In contrast, the PR model gives an excellent agreement with the calculated I_a from Eq. (31).

TABLE VI. Simulation results for the integral (33) at $\rho_r=1$ and $T_r=1.05$.

Model	$\log I_a$
PRH	1.51 ± 0.04
PR	1.18 ± 0.03
CSJ	0.86 ± 0.02
Experimental	1.20 ± 0.20

The comparison of Tables V and VI suggests that the PR-SPC aqueous electrolyte model describes quite reasonably the ion pairing at this near-critical condition. The agreement between the simulation and experimental values of I_a also suggests that care must be exercised in choosing the property used to test the realism with which the model describes the ion-pairing and related solvation phenomena. The inspection of Tables V and VI supports our contention that a direct comparison between K_a^M values from experiment and simulation can be misleading when assessing the realism of models because the uncertainties introduced by the constant of integration overshadow the accuracy of the mean-force calculation.

Finally we compare our results with those from the traditional Bjerrum and Fuoss formalisms to test their accuracy for well defined ion–solvent and ion–ion interaction models. Bjerrum's constant of association K_a^B in units of ℓ/mol and assuming unitary activity coefficients can be written as,[6]

$$K_a^B = 4.0 \times 10^{-3} \pi N_a \left(-\frac{q_{\mathrm{A}} q_{\mathrm{C}}}{kT\epsilon} \right)^3 Q(b), \tag{34}$$

where N_a is Avogadro's number, q is the ion charge in electrons, ϵ is the solvent's dielectric constant, and $Q(b) = \int_2^b x^{-4} e^x dx$ with $x(r) = -(q_{\mathrm{A}} q_{\mathrm{C}}/kT\epsilon r)$, $x(a) = b$ where a is the distance of closest ionic approach, $x(r_{\min})=2$, and $r_{\min} = 0.5ab$ (see the end of Sec. II for details on notation).

Alternatively, Fuoss's formalism describes K_a^F in ℓ/mol by the following expression:[30]

$$K_a^F = (4\pi N_a/3000) a^3 e^b, \tag{35}$$

where $b = -(q_{\mathrm{A}} q_{\mathrm{C}}/kT\epsilon a)$, and a is the sum of the effective radii of the ions in solution, i.e., only those pairs within the spherical shell of volume $4\pi a^3/3$ are counted as paired. Note that this formalism assumes an ionic intermolecular potential of the form,

$$\phi_{\mathrm{AC}} = \frac{q_{\mathrm{A}} q_{\mathrm{C}}}{\epsilon a(1+a\kappa)}, \tag{36}$$

This article is copyrighted as indicated in the article. Reuse of AIP content is subject to the terms at: http://scitation.aip.org/termsconditions. Downloaded to IP:

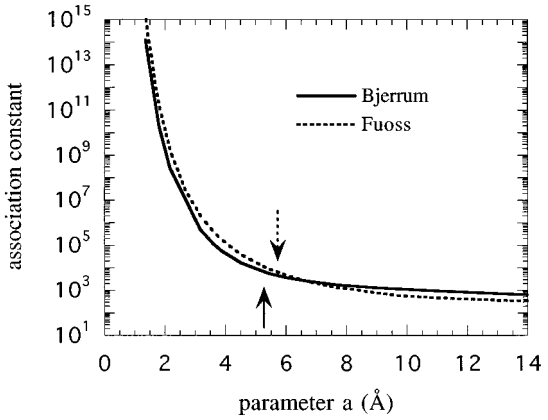

FIG. 7. Dependence of the Bjerrum and Fuoss association constants (in ℓ/mol) on the parameter a. The arrows indicate the values corresponding to the experimental K_a^M at $T_r=1.05$, $\rho_r=1.0$.

where κ^{-1} is the Debye length, and also includes explicitly the contribution of the mean ionic activity coefficient as given by the Debye–Huckel theory, i.e., $\ln \gamma_{\pm}^2 = ab\kappa/(1+a\kappa)$.

The key variable in both theories is the choice of the parameter a, the distance of closest ionic approach, which is typically the result of a regression of experimental data. For our ion–ion potential model, this distance is well defined as the anion–cation soft-core diameter, $\phi(r=a)\approx 0$. Thus, for the Huggins–Mayer–Fumi–Tosi model we have that $a\approx 1.6$ Å so that $K_a^B > 10^{14}$ and $K_a^F > 10^{15}$, while for the PRH model $a\approx 2.2$ Å so that $K_a^B > 10^8$ and $K_a^F > 10^9$. There is no doubt that the Bjerrum and Fuoss expressions do not give accurate estimates for the association constant when the microscopic interpretation of the otherwise adjustable parameter a is used in the calculation. The association constants predicted by these formalisms are extremely sensitive to the value of a as indicated in Fig. 7. This picture indicates that in order to match the experimental value of the association constant, i.e., $K_a^M \approx 6000$, the Bjerrum expression requires a radius $a\approx 5.3$ Å and consequently it considers all ion pairs within the spherical shell with radius $a < r < r_{\min} \approx 26.6$ Å. In contrast, in Fuoss's view only the ion pairs inside the spherical shell of radius $a\approx 5.6$ Å contribute to the association constant.

According to the statistical mechanical interpretation of ion association, Sec. II, Bjerrum's parameters a and $r_{\min}$ correspond to R_L and R_U in Eq. (13), respectively. Bjerrum's values $R_L \approx 5.3$ Å and $R_U \approx 26.6$ Å are beyond the bounds dictated by the microscopic interpretation. Fuoss's values $R_L = 0$ and $R_U \approx 5.6$ Å appear less conflicting with the microscopic picture, provided we recall that this theory considers associated pairs only those in the CIP configuration, in that the CIP configuration for the models studied is defined within the spherical shell of radius $R_U \approx 5$ Å (Note that a new version of Fuoss's theory[61,62] introduces two important changes to the previous one, namely, the parameter a is substituted by $R > a$, the diameter of the Gurney cosphere, and the introduction of a Boltzmann term to account for the SSHIP).

ACKNOWLEDGMENTS

This work was supported by the Division of Chemical Sciences, Office of Basic Energy Sciences, U.S. Department of Energy. The work of HDC, JMS, and REM has been supported by the Division of Chemical Sciences of the U.S. Department of Energy under Contract No. DE-AC-840R21400 with Lockheed Martin Energy Systems, Inc.

APPENDIX

Our simulation results for mean force $F(r)$ and dielectric constant ϵ indicate standard deviations (conservative estimates), $\delta^2 F/\langle F\rangle$ and $\delta^2\epsilon/\langle\epsilon\rangle$ where $\delta^2\varphi \equiv \langle\varphi\rangle^2 - \langle\varphi^2\rangle$, of 10% with respect to their mean values. By taking this as an indication of the uncertainties of the calculated mean values of $F(r)$ and ϵ, then we can estimate the expected errors for the potential of mean force, and consequently the association constants, by running the following Monte Carlo simulation:

(a) Generate random values of $F(r)$ around the simulated means for each distance r, from a uniform distribution in the interval $(-1\leqslant\xi\leqslant 1)$,

$$F(r)_{\text{ran}} = F(r)_{\text{sim}}(1+\xi[\,\delta^2 F/\langle F\rangle]).$$

(b) Compute the difference in the potential of mean force $W_{\text{AC}}(r) - W_{\text{AC}}(r_0)$ thorough the integrands of step (a).

(c) Determine the constant of integration $W_{\text{AC}}(r_0) \approx (q_{\text{A}} q_{\text{C}}/\epsilon r_0)$ by generating a random value for the dielectric constant

$$\epsilon_{\text{ran}} = \epsilon_{\text{sim}}(1+\xi[\,\delta^2\epsilon/\langle\epsilon\rangle]).$$

(d) Determine $g_{\text{AC}}^{\infty}(r)$ and calculate the integrals (13) and (19).

(e) Iterate this procedure 5–20×10^3 times to obtain the sampling statistics.

[1] J. F. Galobardes, D. R. Van Hare, and L. B. Rogers, J. Chem. Eng. Data **26**, 363 (1981).
[2] B. E. Conway, Chem. Soc. Rev. 253, (1992).
[3] G. Y. Markovits and G. R. Choppin, in *Ion Exchange and Solvent Extraction*, edited by J. A. Marinsky and Y. Marcus (Marcel Dekker, New York, 1973), Vol. 3; pp. 51–78.
[4] I. D. Ryabchikov, Phys. Chem. Earth **13-14**, 529 (1981).
[5] J. Brodholt and B. Wood, J. Geophys. Res. **98**, 519 (1993).
[6] Y. Marcus, *Ion Solvation* (Wiley, Chichester, 1985).
[7] L. Haar, J. S. Gallagher, and G. S. Kell, *Steam Tables* (Hemisphere Publishing, New York, 1984).
[8] A. S. Quist and W. L. Marshall, J. Phys. Chem. **72**, 684 (1968).
[9] P. C. Ho, D. A. Palmer, and R. E. Mesmer, J. Solution Chem. **23**, 997 (1994).
[10] J. M. Simonson and D. A. Palmer, Geochimica et Cosmochimica Acta **57**, 1 (1993).
[11] H. F. Holmes and R. E. Mesmer, J. Chem. Thermodyn. **15**, 709 (1983).
[12] R. Wachter and K. Riederer, Pure Appl. Chem. **53**, 1301 (1981).
[13] H. F. Holmes, R. H. Busey, J. M. Simonson, R. E. Mesmer, D. G. Archer, and R. H. Wood, J. Chem. Thermodyn. **19**, 863 (1987).
[14] R. E. Mesmer, D. A. Palmer, and J. M. Simonson, in *Activity Coefficients in Electrolyte Solutions*, 2nd ed., edited by K. S. Pitzer (Chemical Rubber, Boca Raton, 1991), pp. 491–529.
[15] A. I. Mishustin, V. N. Plakhotnik, A. V. Plakhotnik, and E. M. Sukhaya, Russian J. Phys. Chem. **69**, 683 (1995).
[16] J. Barthel and R. Buchner, Chem. Soc. Rev. 263 (1992).
[17] C. W. Davies, *Ion Association* (Butterworths: Washington, 1962).
[18] P. Turq, L. Blum, O. Bernard, and W. Kunz, J. Phys. Chem. **99**, 822 (1995).

This article is copyrighted as indicated in the article. Reuse of AIP content is subject to the terms at: http://scitation.aip.org/termsconditions. Downloaded to IP:

[19] L. X. Dang, J. E. Rice, and P. A. Kollman, J. Chem. Phys. **93**, 7528 (1990).
[20] E. Guàrdia, R. Rey, and J. A. Padró, Chem. Phys. **155**, 187 (1991).
[21] R. Rey and E. Guàrdia, J. Phys. Chem. **96**, 4712 (1992).
[22] S. T. Cui, and J. G. Harris, Chem. Eng. Sci. **49**, 2749 (1994).
[23] J. Gao, J. Phys. Chem. **98**, 6049 (1994).
[24] T. B. Thomason and M. Modell, Hazardous Wastes **1**, 453 (1984).
[25] R. Narayan and M. J. Antal, in *Supercritical Fluid Science and Technology*, edited by K. P. Johnston and J. M. L. Penninger (American Chemical Society, Washington, DC, 1989), Vol. 406; pp. 226–241.
[26] T. M. Seward, Phys. Chem. Earth **13**, 113 (1981).
[27] E. H. Oelkers and H. C. Helgeson, Science **261**, 888 (1993).
[28] M. Eigen and K. Z. Tamm, Elektrochemic **66**, 93 (1962).
[29] S. Winstein, E. Clippinger, A. H. Fainberg, and G. C. Robinson, J. Am. Chem. Soc. **76**, 2597 (1954).
[30] R. A. Robinson and R. H. Stokes, *Electrolytes Solutions*, 2nd ed. (Butterworths, London, 1959).
[31] P. T. Cummings and G. Stell, Mol. Phys. **51**, 253 (1984).
[32] J. Barthel, R. Wachter, and H.-J. Gores, Faraday Discuss. **64**, 285 (1977).
[33] N. K. Bjerrum, Kgl. Dan. Vidensk, Selsk. Mat.-Fys. Medd. **7**, 1 (1926).
[34] A. A. Chialvo, P. T. Cummings, H. D. Cochran, J. M. Simonson, and R. E. Mesmer, in *Innovations in Supercritical Fluids*, edited by K. W. Hutchenson and Neil R. Foster, Symp. Ser. **608**, Chap. 4 (1995).
[35] P. T. Cummings, A. A. Chialvo, and H. D. Cochran, Chem. Eng. Sci. **49**, 2735 (1994).
[36] H. J. C. Berendsen, J. P. M. Postma, W. F. van Gunsteren, and J. Hermans, in *Intermolecular Forces: Proceedings of the Fourteenth Jerusalem Symposium on Quantum Chemistry and Biochemistry*, edited by B. Pullman (Reidel, Dordrecht, 1981), pp. 331.
[37] B. M. Pettitt and P. J. Rossky, J. Chem. Phys. **84**, 5836 (1986).
[38] J. Chandrasekhar, D. C. Spellmeyer, and W. L. Jorgensen, J. Am. Chem. Soc. **106**, 903 (1984).
[39] G. Pálinkás, W. O. Riede, and K. Heinzinger, Zeitschrift für Naturforschung **32**, 1137 (1977).
[40] P. T. Cummings, H. D. Cochran, J. M. Simonson, R. E. Mesmer, and S. Karaborni, J. Chem. Phys. **94**, 5606 (1991).
[41] H. D. Cochran, P. T. Cummings, and S. Karaborni, Fluid Phase Equilibria **71**, 1 (1992).
[42] A. A. Chialvo, P. T. Cummings, and H. D. Cochran, Int. J. Thermophys. (in press).
[43] H. J. Strauch and P. T. Cummings, Fluid Phase Equilibria **83**, 213 (1993).
[44] J. P. Hansen and I. R. McDonald, *Theory of Simple Liquids*, 2nd. ed. (Academic, New York, 1986).
[45] F. G. Fumi and M. P. Tosi, J. Phys. Chem. Solids **25**, 31 (1964).
[46] M. P. Tosi and F. G. Fumi, J. Phys. Chem. Solids **25**, 45 (1964).
[47] C. L. Kong, J. Chem. Phys. **59**, 2464 (1973).
[48] C. W. Gear, Argonne National Laboratory, 1966.
[49] B. J. Palmer, J. Comput. Phys. **104**, 470 (1993).
[50] J. J. de Pablo, J. M. Prausnitz, H. J. Strauch, and P. T. Cummings, J. Chem. Phys. **93**, 7355 (1991).
[51] M. P. Allen and D. J. Tildesley, *Computer Simulation of Liquids* (Oxford University Press, Oxford), 1987.
[52] O. Steinhauser, Mol. Phys. **45**, 335 (1982).
[53] W. L. Jorgensen and C. J. Ravimohan, J. Chem. Phys. **83**, 3050 (1985).
[54] G. Ciccotti, M. Ferrario, J. T. Hynes, and R. Kapral, Chem. Phys. **129**, 241 (1989).
[55] M. Mezei and D. L. Beveridge, Ann. New York Acad. Sci. **482**, 1 (1986).
[56] D. E. Smith and A. D. J. Haymet, J. Chem. Phys. **96**, 8450 (1992).
[57] J. S. Høye and G. Stell, Faraday Discussions Chem. Soc. **64**, 16 (1977).
[58] R. E. Mesmer, W. L. Marshall, D. A. Palmer, J. M. Simonson and H. F. Holmes, J. Solut. Chem. **17**, 699 (1988).
[59] T. Shedlovsky, J. Franflin Institute **225**, 739 (1938).
[60] J. K. Fogo, S. W. Benson, and C. S. Copeland, J. Chem. Phys. **22**, 212 (1954).
[61] R. M. Fuoss, Proc. of the National Academic of Science. USA **75**, 16 (1978).
[62] R. M. Fuoss, J. Am. Chem. Soc. **100**, 5576 (1978).

This article is copyrighted as indicated in the article. Reuse of AIP content is subject to the terms at: http://scitation.aip.org/termsconditions. Downloaded to IP: